Evaluating the Hydrological Cycle over Land Using the Newly-Corrected Precipitation Climatology from the Global Precipitation Climatology Centre (GPCC)

Udo Schneider *, Peter Finger, Anja Meyer-Christoffer, Elke Rustemeier, Markus Ziese and Andreas Becker

Global Precipitation Climatology Centre (GPCC), Deutscher Wetterdienst, Offenbach 63067, Germany; peter.finger@dwd.de (P.F.); anja.meyer-christoffer@dwd.de (A.M.-C.); elke.rustemeier@dwd.de (E.R.); markus.ziese@dwd.de (M.Z.); andreas.becker@dwd.de (A.B.)

* Correspondence: udo.schneider@dwd.de; Tel.: +49-69-8062-2766

Abstract: The 2015 release of the precipitation climatology from the Global Precipitation Climatology Centre (GPCC) for 1951–2000, based on climatological normals of about 75,100 rain gauges, allows for quantification of mean land surface precipitation as part of the global water cycle. In GPCC's 2011-release, a bulk climatological correction was applied to compensate for gauge undercatch. In this paper we derive an improved correction approach based on the synoptic weather reports for the period 1982–2015. The compared results show that the climatological approach tends to overestimate the correction for Central and Eastern Europe, especially in the northern winter, and in other regions throughout the year. Applying the mean weather-dependent correction to the GPCC's uncorrected precipitation climatology for 1951–2000 gives a value of 854.7 mm of precipitation per year (excluding Antarctica) or 790 mm for the global land surface. The warming of nearly 1 K relative to pre-industrial temperatures is expected to be accompanied by a 2%–3% increase in global (land and ocean) precipitation. However, a comparison of climatology for 30-year reference periods from 1931–1960 up to 1981–2010 reveals no significant trend for land surface precipitation. This may be caused by the large variability of precipitation, the varying data coverage over time and other issues related to the sampling of rain-gauge networks. The GPCC continues to enlarge and further improve the quality of its database, and will generate precipitation analyses with homogeneous data coverage over time. Another way to reduce the sampling issues is the combination of rain gauge-based analyses with remote sensing (i.e., satellite or radar) datasets.

Keywords: global precipitation; global water cycle; climate change; rain-gauge undercatch correction

1. Introduction

Gridded data sets of long-term mean (climatological) precipitation help to quantify the mean characteristics of the global water and energy cycle and its changes in the context of climate change. In December 2011, the Global Precipitation Climatology Centre (GPCC) released the previous version of its precipitation climatology [1], based on climatological normals of about 67,200 stations and came up with a (at that time) best estimate for the mean precipitation over the global land surface of 786 mm per year [2].

Since then, the GPCC has further improved and enhanced its database by adding, besides an additional level of quality-control, more precipitation data, so that the most recent release of the precipitation climatology dataset [3] is based on about 75,100 stations with climatological normals in the GPCC's database (see Section 2).

The most recent (2015) and prior release (2011) of the precipitation climatology dataset for the period 1951–2000 are compared to each other with regard to the global average in Section 3.2 and the spatial distribution of the differences is discussed. In Section 3.3, the variations of precipitation over time are studied by comparing the precipitation climatology data for the consecutive, partly overlapping, 30-year reference periods from 1931–1960 up to 1981–2010.

Rain gauge measurements are affected by the systematic gauge-measuring error (Section 4), which is a general undercatch of the true precipitation caused by wind drift over the gauge orifice (most pronounced for snowfall and small droplets), evaporation from the gauge, and wetting losses [4,5]. Besides the features of the instrument, the systematic gauge-measuring error is dependent on the meteorological conditions and the precipitation phase [6,7].

In 1990, Legates and Willmott (hereafter referred to as L&W1990) evaluated a station-based correction for the systematic gauge measuring-error on a global scale for climatological conditions [8]. Some studies [6,7] showed that L&W1990's bulk correction tended to overestimate the systematic gauge-measuring error, i.e., for the areas of the following three experiments of the GEWEX (Global Energy and Water Cycle Exchanges Project) Hydroclimatology Panel (GHP): the Baltic Sea Experiment (BALTEX), the GEWEX Asian Monsoon Experiment (GAME), and the Large-scale Biosphere-Atmosphere (LBA) Experiment in Amazonia. Therefore, only 85% of the correction from L&W1990 has been applied in [2]. Since the bulk climatological correction was identified as the largest uncertainty in the previous estimation of the global mean land surface precipitation from the GPCC's precipitation climatology, we replaced it by using an improved weather-dependent correction approach.

The methodology to correct the systematic gauge-measuring error on the basis of weather information from synoptic stations, thereby taking the weather conditions in the observation period into account, was developed by [7,9]. This method was then implemented at the GPCC [6] and allowed for the calculation of weather-dependent correction for the systematic gauge-measuring error by using the synoptic weather reports exchanged via the Global Telecommunication System (GTS) of the WMO (World Meteorological Organization) that are received at the Deutscher Wetterdienst (DWD, German Weather Service) in Offenbach. The GPCC started these evaluations in 2007, but so far, the use of this improved approach has been hampered for not being available retrospectively.

The GPCC undertook the large effort of re-assessing the synoptic weather reports back to 1982 based on the methodology according to [6]. This now allows an improved assessment of the correction for the gauge undercatch, taking into account the weather conditions (inter alia), as well as the precipitation phase (liquid, mixed, solid) for each individual day in the entire period since 1982 (for details see Section 4). The improved undercatch correction reduces the uncertainty in the bias correction and thereby improves the quality of the GPCC's precipitation climatology, as well as of the other precipitation data products described in [10,11].

After having presented the new GPCC undercatch correction for the period 1982–2015 (based on SYNOP weather reports) in Section 5 it will be discussed how the mean precipitation over land derived from GPCC's new precipitation climatology fits into the larger picture of the global water cycle as described in [12–14] and how the variations over the different 30-year periods compare to the expected changes in the global water cycle in the context of climate change [15].

2. GPCC's Data Base

Since the 2011-release of its precipitation climatology [1] described in [2] the GPCC has further enhanced its database. Updates for many countries have been integrated and a significant amount of data has been added for Brazil, Colombia, Mexico and some previously data sparse regions (i.e., for Ethiopia, Libya, Somalia, the Lake Chad region, Cambodia, and Kyrgyzstan). The database has also been significantly enhanced for Indonesia and for other island/atoll regions (Bahamas, Caribbean Islands, French Polynesia, Mauritius, Reunion, Seychelles and Vanuatu). Figure 1 shows

the contribution of the different data sources that the GPCC archives separately in source-specific slots in its relational database management system (for more details see [2]).
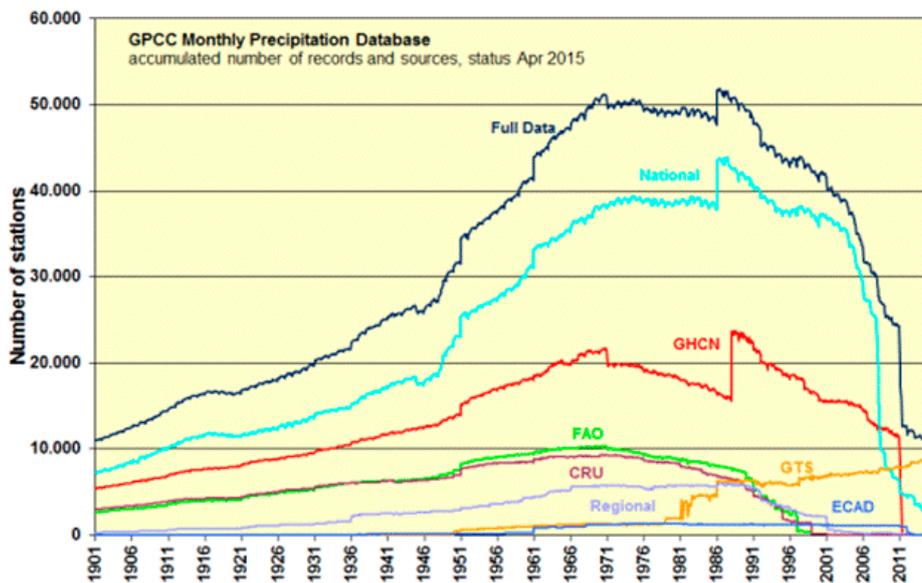
Figure 1. Total number of stations with monthly precipitation data over time (shown since 1901) in the Full Data Base of the Global Precipitation Climatology Centre (GPCC) according to the different data sources.

The new 2015 release of the precipitation climatology for the period 1951–2000 is now based on approximately 75,100 stations with climatological normals in the GPCC database; their spatial distribution is shown in Figure 2.
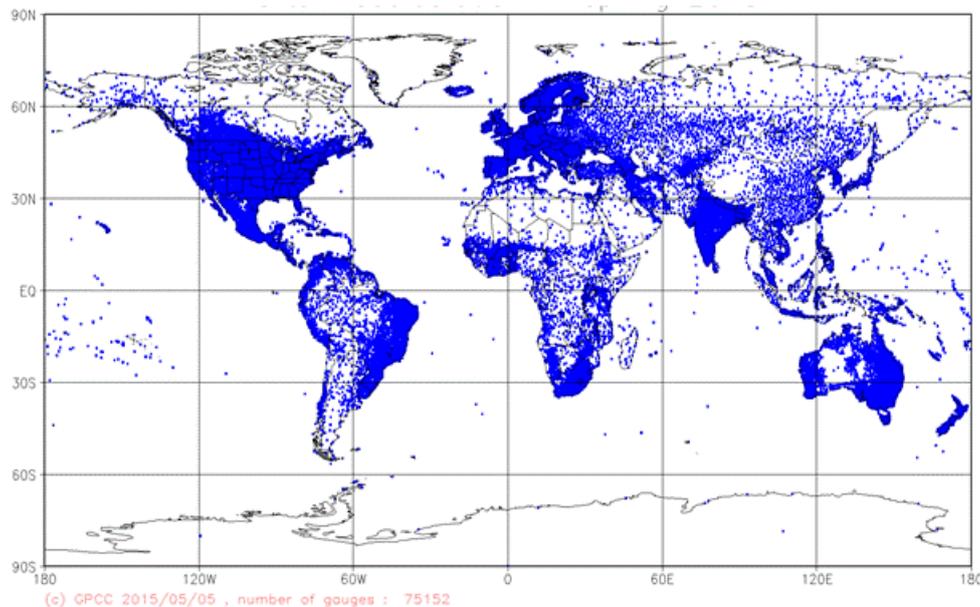
Figure 2. Spatial distribution of monthly in-situ stations with a climatological precipitation normal in the GPCC database (number of stations in July: 75,152).

The quality-control (QC) processing of the Full Data Base of the GPCC described in [2] has been repeated for the new release, and the data screening has been further improved.

Verifying the locations for the additional island/atoll regions mentioned before in the process of integrating the station data into GPCC's database management system revealed that the old, much coarser land mask was missing a considerable number of islands/atolls. Therefore, a significantly improved land mask was constructed by combining those of the Global Land Data Assimilation System (GLDAS) [16] and the International Satellite Land-Surface Climatology Project Initiative II (ISLSCP II) [17].

3. The New 2015 Release of Precipitation Climatology from the GPCC and Comparison to the 2011 Release

3.1. New 2015 Release of GPCC's Precipitation Climatology

As described in [2] for the 2011-release, the new 2015 version of the Global Precipitation Climatology [3]keeps its focus on the reference period 1951–2000, but now consists of normals from about 75,100 stations, constituting an increase of almost 8000 climatology-relevant stations. The climatology comprises normals collected by the WMO [18], delivered by the countries to GPCC or calculated from the time-series of monthly data available in the GPCC database.

In the case that time series of sufficient lengths (at least 40 years) for the period 1951–2000 were not available from a specific station, climatological normals were also been calculated for 30-year reference periods within the period 1951–2000 (for 1961–1990, 1951–1980 or 1971–2000) with at least 20 years of data. If even this was not possible for a station, then normals were calculated for other 30-year periods: 1931–1960, 1941–1970 or 1981–2010 or for any other period with at least 10 complete years of data. Figure 3 displays the climatological mean precipitation for July as an example.
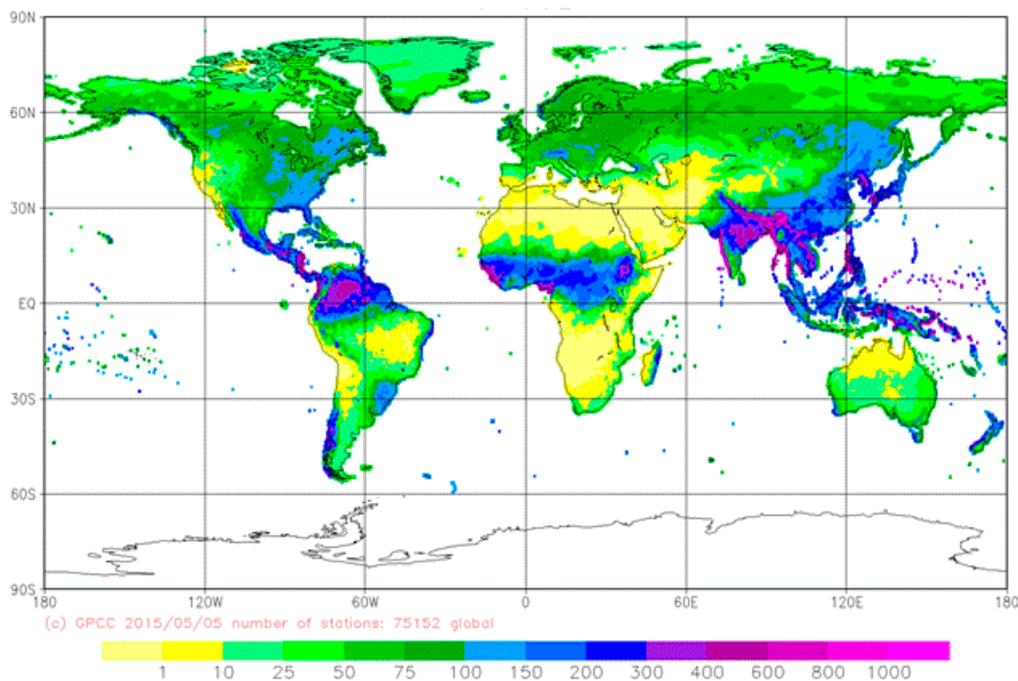
Figure 3. Climatological mean precipitation for July based on new Global Precipitation Climatology (Version 2015) from the GPCC, focusing on the period 1951–2000, 0.25° × 0.25° resolution).

3.2. Comparison of the 2015 Release to the 2011 Release

A significantly improved land mask was constructed by combining the land masks of GLDAS [16] and ISLSCP II [17]; in addition, island stations missing in both land masks have been added after a manual check of the station location with other geographical information sources.

Not surprisingly, the differences between the two releases of the GPCC's precipitation climatology are largest where significant amounts of station data have been added, as illustrated by Figure 4a–c showing the absolute differences (mm) between the 2015 and 2011 releases of the climatology for January, July, and the entire year. While there are larger, but mostly spotty, differences in the individual months across regions like Brazil, Colombia, Mexico and Indonesia where significant amounts of station data have been added (see Figure 4a,b), the differences over the year are generally small (Figure 4c). Notwithstanding, the annual differences are only significant across Mexico, western Colombia and Indonesia.

Figure 4c also indicates the significant enhancement of the new land mask utilized in the 2015 release by highlighting (in dark blue) the differences with respect to the coarser 2011 version, mainly adding a lot of islands/atolls that were missing in the old land mask.

The average annual total precipitation value—without correction for the gauge-undercatch error that will be discussed in Section 4—over the land surface for 1951–2000 is now 793.6 mm, with a 0.5° spatial resolution (based on 75,100 stations), which is slightly higher than in the 2011 release with a value of 791.8 mm (based on 67,200 stations). Due to the, in general, small-scale nature of extreme precipitation events, a denser (coarser) station network enhances the chances to catch (miss) such extreme events, leading to a tendency towards slightly higher precipitation values with an increasing number of stations in the precipitation climatology, in particular in regions with an abundance of convection.
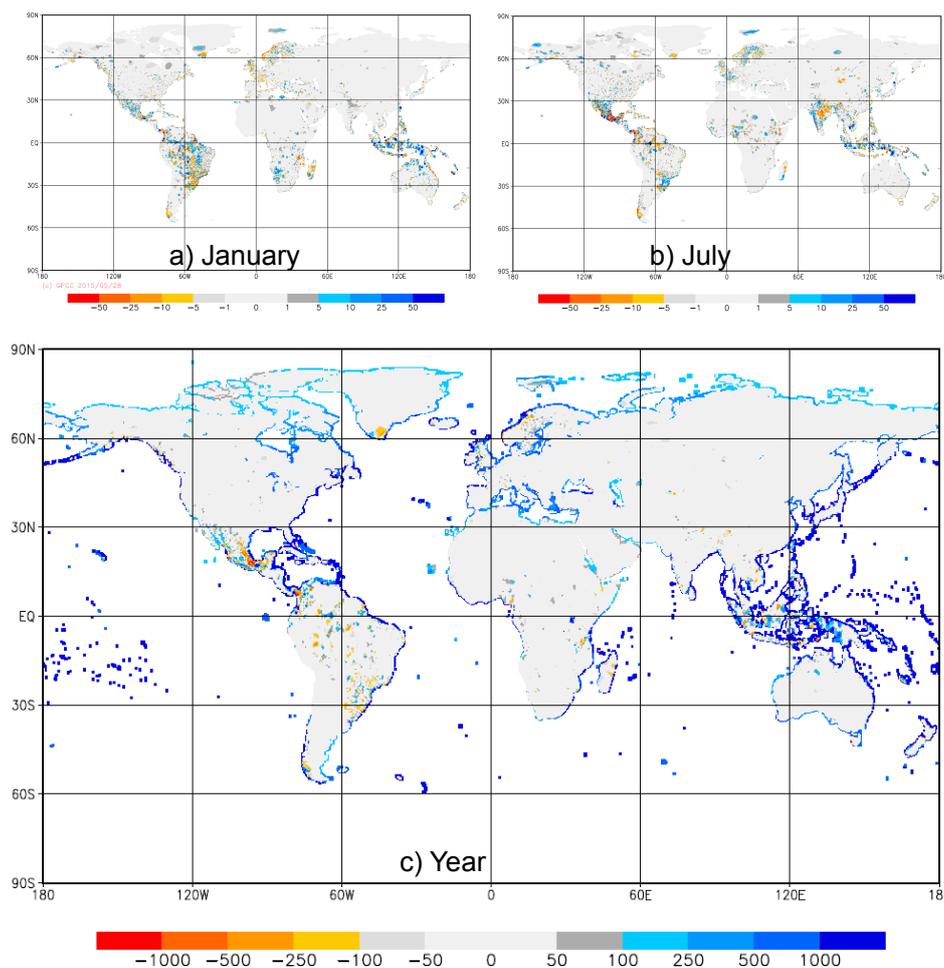
Figure 4. Differences (mm) between the 2015 release of GPCC's precipitation climatology and the 2011 release for (**a**) January; (**b**) July and (**c**) for the year. The map for the year (**c**) also highlights the differences of the land masks (dark blue) between the two releases.

3.3. Variations of Mean Precipitation over Different Reference Periods

In this section, the consecutive 30-year reference periods from 1931–1960 to 1981–2010 are compared to the GPCC's 50-year precipitation climatology 1951–2000, and the differences are shown in Figure 5. Red/blue areas indicate less/more precipitation in the 30-year periods than in the 50-year period 1951–2000.
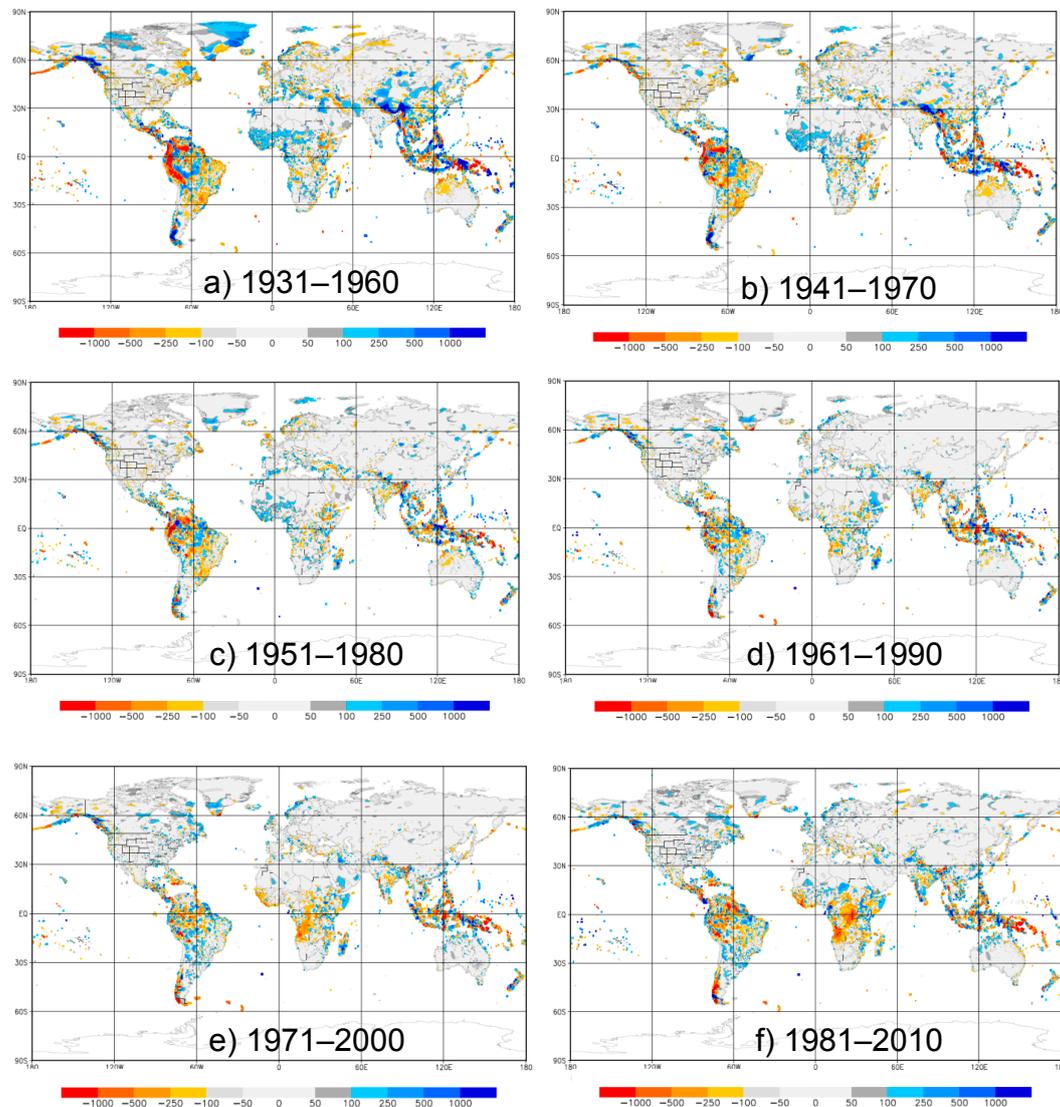

Figure 5. Differences between mean annual precipitation for the different 30-year reference periods (**a**) 1931–1960; (**b**) 1941–1970; (**c**) 1951–1980; (**d**) 1961–1990; (**e**) 1971–2000 and (**f**) 1981–2010 to GPCC's precipitation climatology 1951–2000 [3].

In the periods 1931–1960 and 1941–1970, there are larger differences compared to the 1951–2000 precipitation climatology over South America, where it is drier, particularly over the Andes. More rainfall occurred during both periods over West Africa (including Sahel) whereas contrasting deviations are found over Southeast Asia and especially Indonesia. The positive differences over the Tibetan/Himalayan region are probably caused by the interpolation of the scarce data in the topographically highly structured region in these early periods. In 1931–1960 more precipitation was observed across the anyway very humid Alaska panhandle.

The positive rainfall anomalies observed over West Africa in the early periods decreased in the period 1951–1980, and diminished thereafter. This reflects the long-term precipitation variations over West Africa and Sahel described by Nicholson [19,20]. The negative anomalies in Central Africa for 1971–2000 and 1981–2010 are not reliable; especially over Angola and the Democratic Republic of Congo; this may be due to the absence or scarcity of data over the last decades.

The Hovmoeller diagrams in Figure 6 show the mean annual cycle of the climatological zonal mean precipitation for 1951–2000 (leftmost) in comparison to the other six 30-year reference periods analysed with decadal updates starting from 1931–1960. Most obvious is the weak but steady increase of observed precipitation at northern hemispheric high latitudes. Part of this may be obscured by the very scarce data coverage over Greenland (there are only a few precipitation stations at the coast, but none inland), but part of this may be real and caused by the increase in temperature at high latitudes. A combination of factors might have caused this: the increased temperatures reducing sea ice coverage, especially in summer, will result in more evaporation from open water. Moreover, an increased fraction of liquid and mixed precipitation phase with increasing temperatures might also have factored in. The observed increase is in agreement with the increased precipitation found in model simulations in high latitudes, particularly in the northern winter [21]. Over the high southern latitudes precipitation has decreased over the more recent decades since 1961–1990, which is reflected in Figure 5 in the decreased precipitation in particular over southern Chile (negative anomalies).
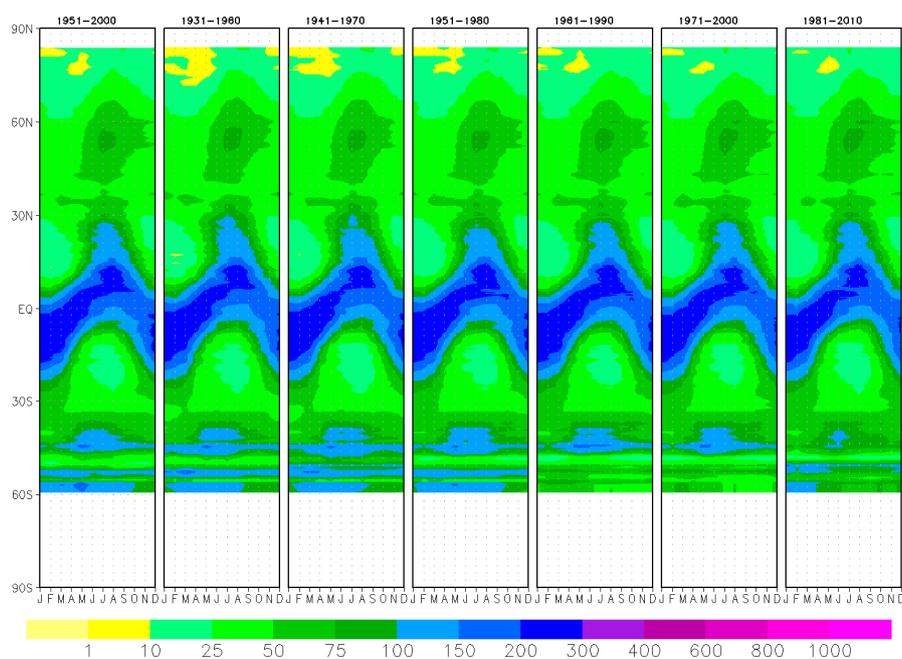
Figure 6. Hovmoeller diagram of zonal mean precipitation (mm/month) over the year for (left) GPCC's precipitation climatology 1951–2000, and the different 30-year reference periods (second-left to right) 1931–1960, 1941–1970, 1951–1980, 1961–1990, 1971–2000 and 1981–2010.

The summer maximum, related to the Asian summer monsoon, seems to be slightly reduced during the most recent 30-year reference periods. One reason might be the more frequent occurrence of El Niño/Southern Oscillation (ENSO) events during the last decades, which generally are accompanied by a weakened Indian and South East Asian summer monsoon [22,23].

Figure 7 shows the mean annual cycle for the global land surface for the reference periods 1931–1960 to 1981–2010. The mean precipitation varied between 58 and 64 mm per month from January to May, increased up to about 68 mm in June and reached a maximum of 78 to 79 mm in July and August caused by the Asian summer monsoon. Thereafter, the mean precipitation decreased with a minimum of about 58 mm in November.
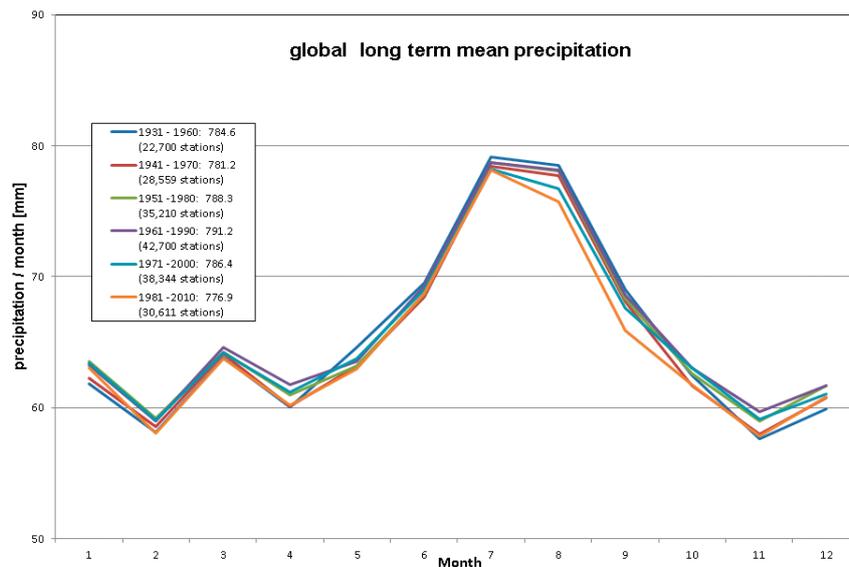
Figure 7. Mean annual cycle over the global land surface for the different 30-year reference periods 1931–1960, 1941–1970, 1951–1980, 1961–1990, 1971–2000 and 1981–2010.

While the annual precipitation is lower in the early periods 1931–1960 and 1941–1970 with 784.6 and 781.2 mm, respectively, it increases through 1951–1980 (788.3 mm) to 1961–1990, with 791.2 mm. Over the recent reference periods it decreased to 786.4 mm (1971–2000) and only 776.9 mm in 1981–2010. From Figure 7 it can be seen that precipitation decreased in the most recent reference periods in particular in August, September and October which might, as mentioned before, be related to a more frequent occurrence of ENSO events during the last decades being often accompanied by a weakened Indian and Southeast Asian summer monsoon. The numbers of climatological normals for the different reference periods are also given in Figure 7, increasing from only 22,700 for 1931–1960 up to a maximum of 42,700 for 1961–1990, and decreasing to 38,344 and 30,611 for 1971–2000 and 1981–2010, respectively. As mentioned above, due to the general small-scale nature of extreme precipitation events, the reference period specific number (and spatial distribution) of stations has an effect on the corresponding global averages that is hard to quantify and will be discussed in the conclusions.

4. Weather-Dependent Correction of the Systematic Gauge-Measuring Error for 1982–2015

The methodology described in [7,9] was implemented at the GPCC [6] and allows for the calculation of a weather-dependent correction for the systematic gauge-measuring (undercatch) error by using the synoptic weather reports exchanged via the WMO's Global Telecommunication System (GTS) that are received at Deutscher Wetterdienst (DWD) in Offenbach.

Previously, the improved undercatch correction factors had been available at GPCC only from 2007 onwards; to overcome the uncertainties of the bulk climatological correction L&W1990 [8] the GPCC evaluated the SYNOP reports for the entire period back to 1982; before that the synoptic station database was too poor to provide reliable results.

The weather-dependent correction of the systematic gauge-measuring error for 1982 to 2015 is calculated on the basis of the method using the weather information from the SYNOP stations distributed via WMO's GTS system [6,7,9]. The weather information from the SYNOP reports has been first aggregated for the day and finally over the month to provide the monthly correction factors for each station. Finally, the monthly correction has been interpolated for a 0.5° grid by using the modified SPHEREMAP method described in [10], also used in the interpolation for GPCC's gridded monthly precipitation datasets. Figure 8 shows the correction factors for compensating the systematic gauge-measuring error for the GPCC method (left) averaged for the period 1982–2015 and (right) from L&W1990 for January, April, July and October. Owing to significant errors in the SYNOP reports

for some Greenland stations in December 2013, January, October and December 2014, and January to April 2015, the results for the gauge-measuring error had to be ignored across Greenland during these months.
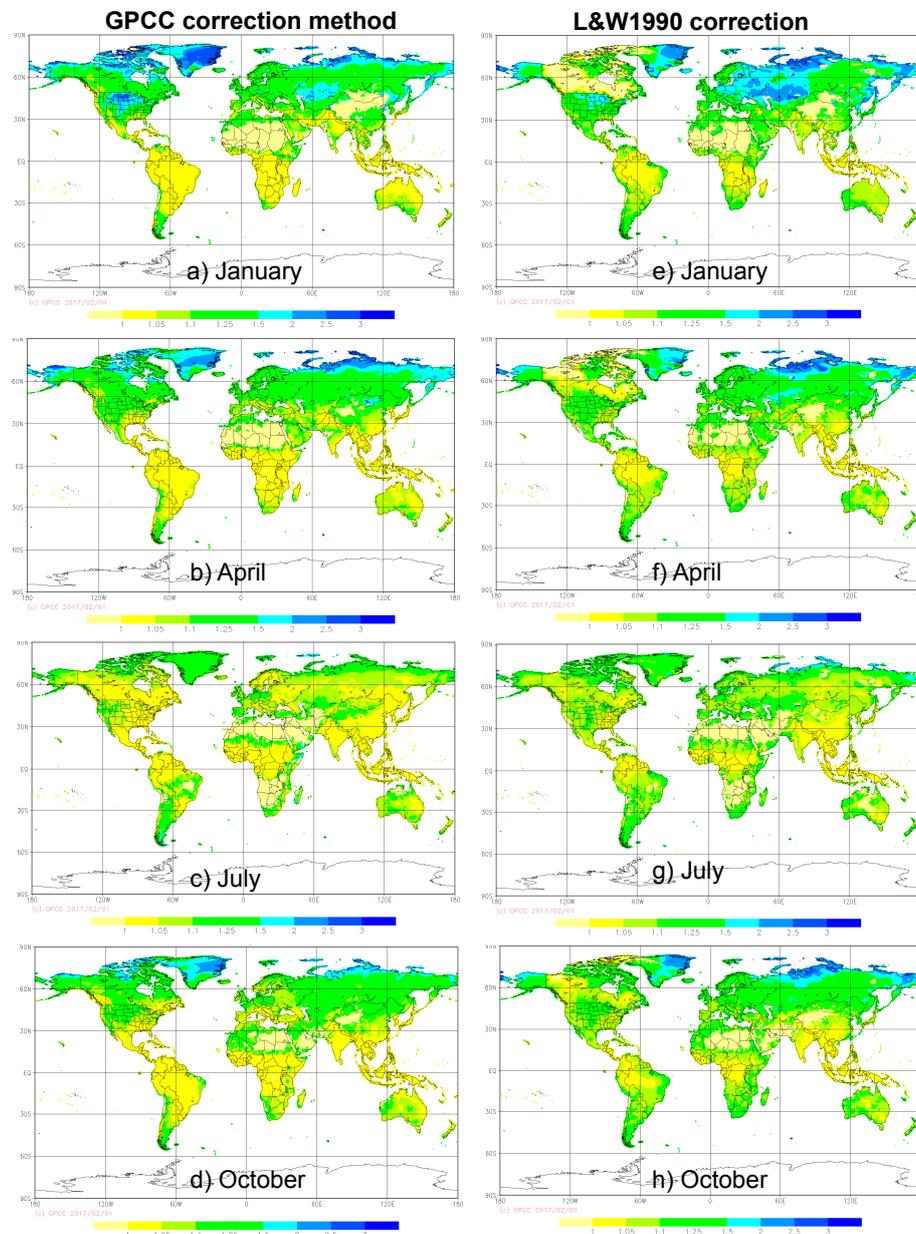
Figure 8. Mean correction factors from (**left**) GPCC correction method averaged for 1982–2015 for January, April, July and October and (**right**) Legates and Willmott (L&W1990, [8]) for the same months.

In Figure 9 the absolute differences (in mm) between the GPCC's correction (according to [6]) averaged for the period 1982–2015 and from L&W1990 are shown for January, April, July and October and for the year. It is obvious that the L&W1990 bulk correction results in too high correction values for Central and Eastern Europe, including the BALTEX area, especially in the northern winter, which is in agreement with the findings for the years 1996 and 1997 [6,7]. L&W1990 also overestimate the gauge-correction in Central and Southern Africa, and over all of South and Central America, including the LBA region throughout the year (also in agreement with [7]). Over Canada, however, L&W1990 has almost no correction and significantly underestimate the systematic gauge-measuring error.
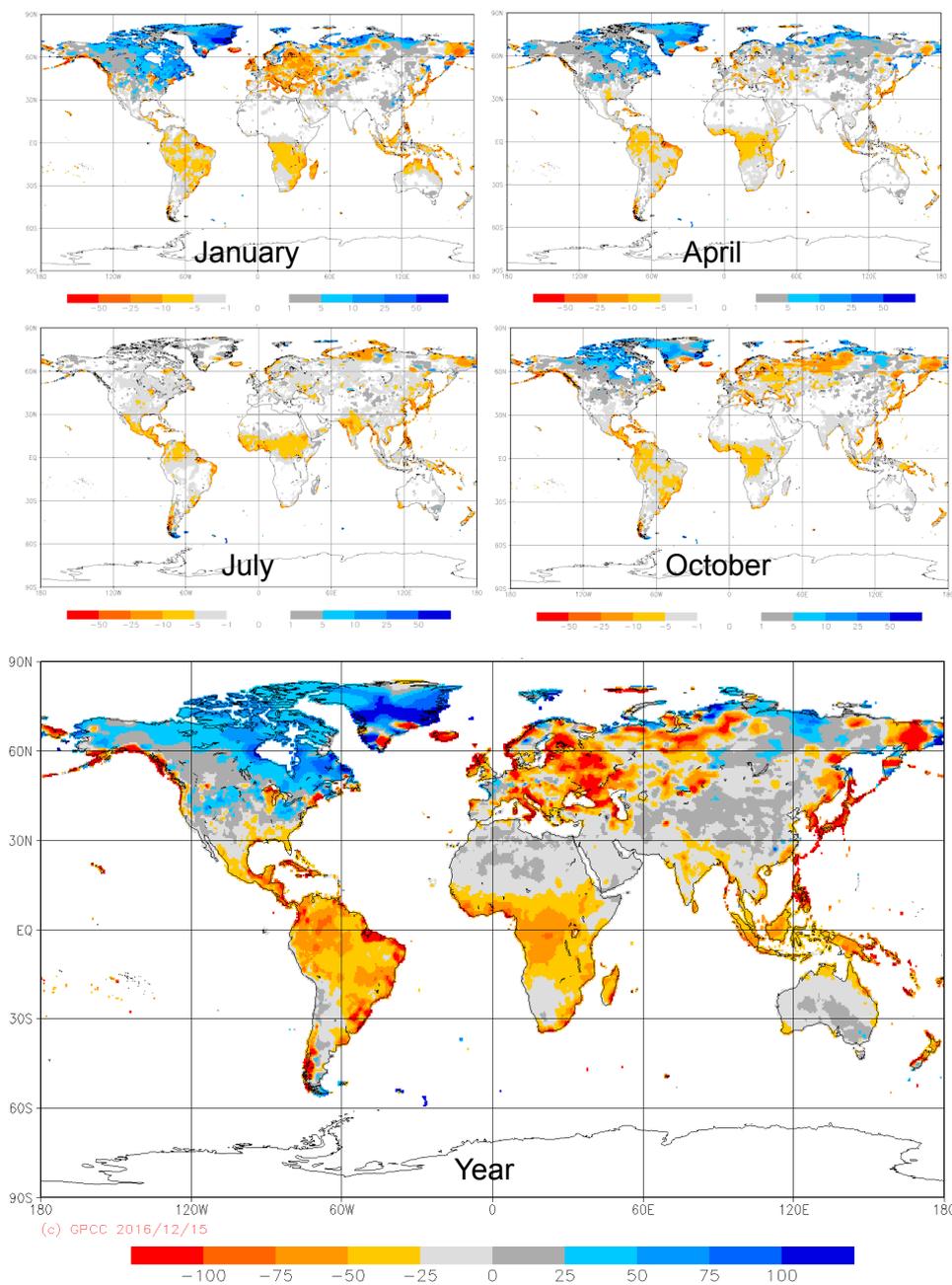
Figure 9. Absolute differences (mm) between correction terms for the systematic gauge-measuring error according to GPCC and L&W1990 for January, April, July, October and the year.

From L&W1990, there are two different dataset versions available, one as measured, and the other including a correction for the gauge undercatch. Therefore, the correction can be calculated in two different ways, as an additive correction term (the difference between both versions) or as a correction factor-derived as ratio of the corrected dataset to the measured one.

A simple example illustrates why application of the additive approach is not recommended: A correction of 5 mm with a measured precipitation of 50 mm (10%) in any place around the world in a given month (i.e., January) could lead to an unrealistically high/low correction of 50%/5% for dry/wet conditions, respectively with 10 mm/100 mm of precipitation in another January in the same place. However, applying the correction factor at 10% always will give a more realistic correction, (1 mm or 10 mm for the dry/wet conditions, respectively). Therefore, we strongly recommend utilizing

the approach using the correction factors, as it is applied in the datasets of the Global Precipitation Climatology Project (GPCP) [24,25].

The monthly correction factors for the systematic gauge-measuring error, as well as the precipitation phase (liquid, mixed or solid), are provided in conjunction with the monthly precipitation data of the GPCC's Monitoring Product available via GPCC's homepage.

Figure 10 shows the average portion of the precipitation phases (liquid, solid, mixed) over the entire period 1982–2015.
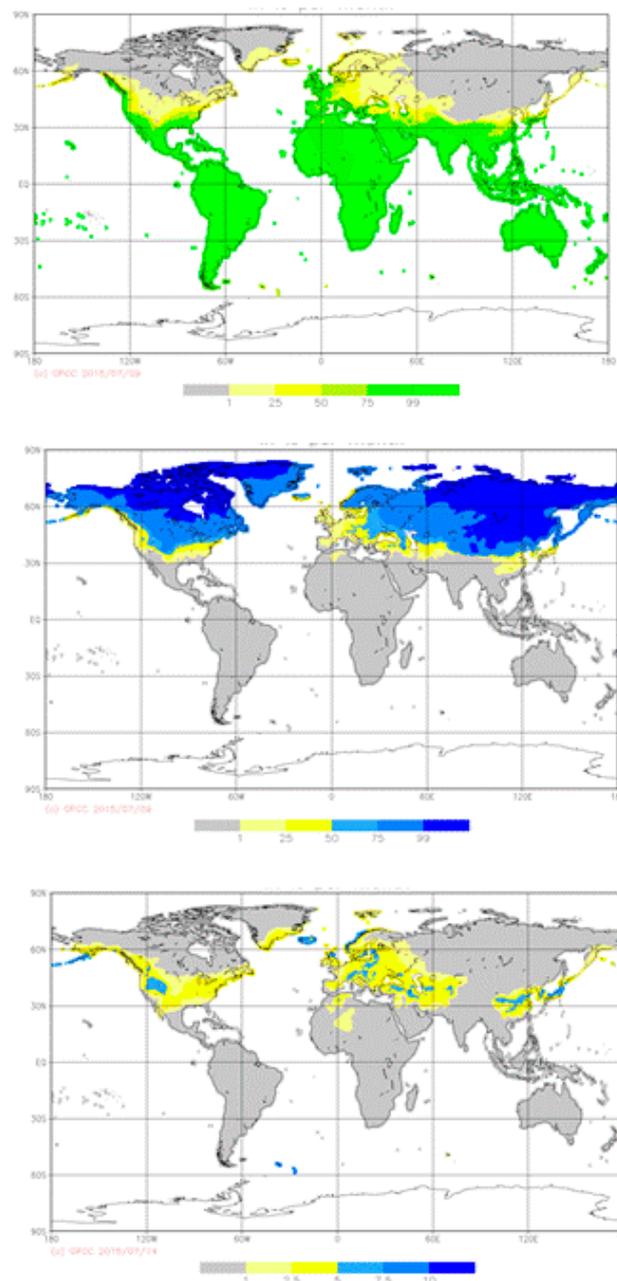
Figure 10. Example of the mean percentage of precipitation phases for January over the period 1982–2015 (**top**) liquid, (**middle**) solid and (**bottom**) mixed phase.

Averaging the GPCC's land surface weather-dependent correction month-by-month for the global land surface (excluding Antarctica) and over the entire period 1982–2015 provides the mean correction factors in Table 1 for each calendar month and the entire year.

Table 1. Mean (GPCC) and mean corrected (GPCC Corr.) precipitation totals over the period 1982–2015 for the calendar months and the year, as well as mean correction factors for the systematic gauge-measuring error utilizing the weather information.

	January	February	March	April	May	June	July	August	September	October	November	December	Year
GPCC	64.1	59.6	65.0	61.7	63.8	69.1	78.9	77.7	68.8	63.2	59.6	62.3	800.9
GPCC Corr.	69.4	64.3	69.6	65.6	66.9	71.9	81.7	80.4	71.6	66.8	64.1	67.5	862.3
Mean Correction Factor	1.083	1.078	1.070	1.063	1.049	1.040	1.036	1.035	1.040	1.058	1.079	1.084	1.077

The correction factors for the global land surface averaged over the entire period 1982–2015 vary between only 1.035 and 1.04 (correction of 3.5% to 4%) in summer (June to September), but are highest in winter with 1.083 to 1.084 (correction of 8.3% to 8.4%) in December and January. On average, the correction for the year is 7.7%, somewhat lower than the 8.9% of L&W1990 [8], but in the same range if 85% of L&W1990's correction is applied [2] yielding an average correction of 7.56%. It should be kept in mind that the relative gauge undercatch can be significantly higher than the average in northern high latitudes (i.e., snowfall), where it is often relatively dry (up to 50% or more than 100% in individual events), whereas it is relatively small for most low-latitude regions.

Lacking further information about the weather-dependent correction factors before 1982, we applied the weather-dependent correction factor 1.077 derived from the synoptic weather reports for the period 1982–2015 to the GPCC's precipitation climatology for the period 1951–2000 (793.6 mm per year). This led to an average gauge-corrected land surface precipitation of 854.7 mm per year (excluding Antarctica).

Using the estimate for Antarctica of 166 mm per year based on net surface mass balance [26] results in a mean precipitation estimate for the total land surface (incl. Antarctica) of 790 mm (area weighting according to Table 2 in [2]. In the next chapter it will be discussed how this fits into the global water cycle.

5. The Hydrological Cycle over Land as Evaluated from the GPCC's New Gauge-Corrected Precipitation Climatology

The oceanic and terrestrial water exchanges (transports) as part of the hydrological cycle are converted into volumetric sizes of precipitation and evaporation by using the areal extents for the land, ocean and global surface from Table 2 in [2].

A global land surface precipitation (for the period 1951–2000) of 790 mm is equivalent to a water transport of 117,600 km^3 per year. This is slightly higher than the estimates of 117,000 km^3 per year derived from GPCC's previous climatology dataset [2] or the 116,500 km^3 per year for the early 20th century evaluated on the basis of a closure of the water and energy budget [14].

While the previous estimate of the Global Runoff Data Centre (GRDC, 2009) for the "global" runoff (excluding Antarctica and Greenland) into the world oceans was only 36,109 km^3 per year [27], the new GRDC estimate [28] is significantly higher, at 41,867 km^3 per year. In contrast to the previous version, the new estimate based on the hydrological model WaterGap 2.2 includes the water runoff for Greenland, being on the order of 420 km^3 per year. Based on the same global hydrological model, authors of [29,30] found runoff estimates of a similar order when taking the correction for the gauge undercatch into account. Since the WaterGap 2.2 model does not include glacier dynamics, we added 280 km^3 per year attributed to iceberg calving in Greenland [31] to the GRDC estimate. Together with a runoff estimate for Antarctica of 2613 km^3 per year [32] this resulted in a total surface runoff of about 44,800 km^3 per year. Lacking other quantitative information for the annual groundwater flow into the oceans we assumed this quantity to be on the order of 1000 km^3, and arrived at a total runoff (rivers and groundwater) of about 45,800 km^3 per year, close to the recent estimate for the global runoff of 45,900 km^3 per year [14].

For continuity reasons, the transport of water vapour by advection from ocean to land has to be of the same order as the total runoff, leading over land to an evapotranspiration of 71,800 km^3 per year. Figure 11 shows the global water exchange quantities for precipitation, evaporation/evapotranspiration separately for ocean and land, respectively. The precipitation over land is derived from the 2015 release of GPCC's climatology. The total runoff of 45,800 km^3 per year is based on the new GRDC estimate [28] plus runoff estimates for Antarctica and Greenland and a groundwater component. The precipitation estimate of 386,000 km^3 per year over the ocean is based on [13,14] and new data from GPCP V2.3 [25]. With the transport of water vapour from ocean to land of 45,800 km^3 per year, the evaporation over the oceans should be 431,800 km^3 per year, and the total

water exchange by precipitation/evapotranspiration can be estimated to be about 503,600 km^3 per year, being equivalent to 987 mm precipitation per year on global average.
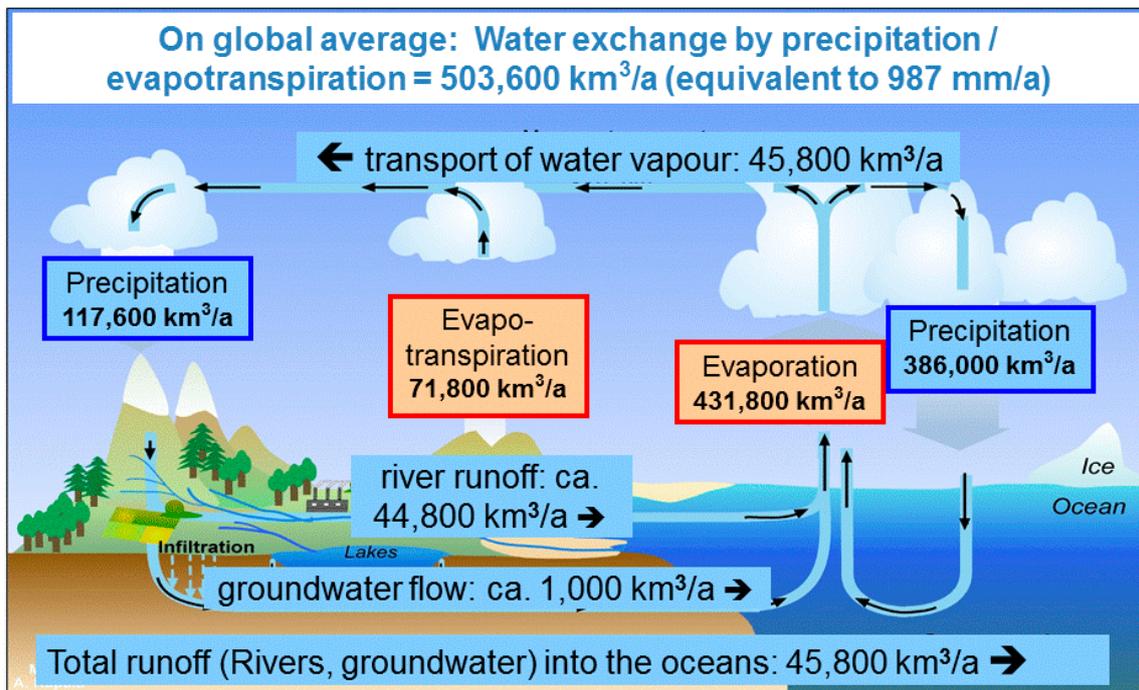
Figure 11. Average water transport/exchanges in km^3 per year as derived from GPCC's precipitation climatology for 1951–2000 land surface precipitation, numbers for precipitation over oceans, evapotranspiration/evaporation over land/ocean taken from [13,14], background picture by courtesy of A. Kapala (Meteorological Institute, University Bonn).

6. Conclusions

To compensate for the systematic gauge-measuring error (a general undercatch of true precipitation by the rain gauges), we derived a weather-dependent correction firstly aggregated on a daily basis and finally averaged for each month of the period 1982–2015 on the basis of weather reports from synoptic stations exchanged via WMO's GTS. These correction factors averaged for each calendar month of the entire period 1982–2015 were then compared to the widely-used bulk correction factors evaluated for climatological conditions [8]. The findings in [6,7] that for the 2 years 1996, 1997 L&W1990's bulk climatological correction tended to overestimate the gauge-measuring error was confirmed in the intercomparison in Section 4. L&W1990 overestimate the gauge-measuring error in Central and Eastern Europe, including the BALTEX area, in particular in the northern winter, and in Central and Southern Africa and over entire South and Central America, including the LBA region, throughout the year. Over Canada, however, L&W1990 have almost no correction and significantly underestimate the systematic gauge-measuring error. This is largely consistent with the findings in [33].

The 2015 release of GPCC's precipitation climatology (not corrected for the gauge undercatch) for the period 1951–2000 (based on climatological normals from about 75,100 stations) gives an average land surface precipitation (excluding Antarctica) of 793.6 mm per year, slightly higher than the 791.8 mm value for the 2011 release (based on 67,200 stations). Lacking any information of the weather-dependent correction before 1982 due to the scarcity of SYNOP data, we applied the mean correction factor of 1.077 derived for 1982–2015 to the GPCC's mean precipitation for the period 1951–2000 (793.6 mm per year). This results in an average precipitation of 854.7 mm per year (excluding Antarctica) or 790 mm per year for the global land surface.

The comparisons of precipitation for the consecutive 30-year reference periods from 1931–1960 up to 1981–2010 revealed no significant overall trend. After a slight increase in annual precipitation from the early periods 1931–1960 and 1941–1970 with 784.6 and 781.2 mm, respectively, to 791.2 mm in 1961–1990, the annual precipitation decreased over the recent reference periods to 786.4 mm (1971–2000) and only 776.9 mm in 1981–2010. Part of these variations probably can be attributed to varying station coverage over time (the numbers of climatological normals varied from 22,700 in 1931–1960 to a maximum of 42,700 in 1961–1990 to 30,611 for 1981–2010). Due to the, in general, small-scale nature of extreme precipitation events, a denser station network is more likely to catch such extreme events, leading to a tendency towards slightly higher precipitation values with an increasing number of stations in the precipitation climatology. Other causes might be variations in the global circulation, for example in the context of a more frequent occurrence of ENSO events during the more recent decades [22,23], or changes related to aerosols [34].

With global warming, evaporation, especially over the oceans, is enhanced, leading to more precipitation. According to the Clausius–Clapeyron relationship per K of warming and energetic constraints an increase in global-mean evaporation and precipitation of 2%–3% can be expected [35], as also demonstrated by climate model simulations [15]. While over oceans a simple relationship between an increase in surface temperature and evaporation/precipitation can be expected, the situation is more difficult over land. The water that is evaporated (E) in excess of precipitation (P) over the oceans (P–E negative) is transported by advection to the land. Besides that, over land an increase in temperature can only trigger more evaporation if enough water is available (soil moisture), but not when the soil has dried out, so the change in precipitation over land might be even less than 2%–3%.

In contrast to global temperature, the energetic constraints for the hydrological cycle are weaker [35]. Therefore, the expected 2%–3% increase in global precipitation (which may be even less over land) is hard to detect given the large variability of precipitation in space and time (small signal-to-noise ratio). In [36], issues with the sampling of rain-gauge networks are discussed and it is vividly pointed out that the pure orifices of all the rain gauges in GPCC's precipitation climatology would cover only about the area of half a soccer pitch (without regarding the spatial representativeness of the gauges).

The GPCC will continue its work to enlarge and further improve the quality of its database to reduce the sampling issues. The problems with the varying data coverage will be overcome with homogenized precipitation analysis for Europe (HOMPRA-Europe) by the GPCC, with quite homogenous data coverage over 1951–2005, which will be available soon, followed later by a second analysis on a global-scale. This will minimize the effects of varying data coverage over time and help to study precipitation trends.

Another way to solve the sampling issues is the combination of GPCC's precipitation analyses with remote-sensing (i.e., satellite or radar) datasets, which have a near-global coverage, as this is done for example with the GPCP datasets [24,25].

The different gridded monthly precipitation datasets of the GPCC are freely available via the GPCC homepage [37].

References

1. Meyer-Christoffer, A.; Becker, A.; Finger, P.; Rudolf, B.; Schneider, U.; Ziese, M. *GPCC Climatology Version 2011 at 0.25°: Monthly Land-Surface Precipitation Climatology for Every Month and the Total Year from Rain-Gauges Built on GTS-Based and Historic Data*; GPCC: Offenbach, Germany, 2011.

2. Schneider, U.; Becker, A.; Finger, P.; Meyer-Christoffer, A.; Ziese, M.; Rudolf, B. GPCC's new land surface precipitation climatology based on quality-controlled in situ data and its role in quantifying the global water cycle. *Theor. Appl. Climatol.* **2014**, *115*, 15–40. [CrossRef]

3. Meyer-Christoffer, A.; Becker, A.; Finger, P.; Rudolf, B.; Schneider, U.; Ziese, M. *GPCC Climatology Version 2015 at 0.25°: Monthly Land-Surface Precipitation Climatology for Every Month and the Total Year from Rain-Gauges Built on GTS-Based and Historic Data*; GPCC: Offenbach, Germany, 2015.

4. Sevruk, B. *Methods of Correction for Systematic Error in Point Precipitation Measurements for Operational Use*; WMO: Geneva, Switzerland, 1982.

5. Sevruk, B. *Correction of Monthly Precipitation for Wetting Losses*; WMO: Geneva, Switzerland, 1985; pp. 7–12.

6. Fuchs, T.; Rapp, J.; Rubel, F.; Rudolf, B. Correction of Synoptic Precipitation Observations due to Systematic Measuring Errors with Special Regard to Precipitation Phases. *Phys. Chem. Earth B* **2001**, *26*, 689–693. [CrossRef]

7. Ungersböck, M.; Rubel, F.; Fuchs, T.; Rudolf, B. Bias Correction of Global Daily Rain Gauge Measurements. *Phys. Chem. Earth B* **2001**, *26*, 411–414. [CrossRef]

8. Legates, D.R.; Willmott, C.J. Mean seasonal and spatial variability in gauge-corrected, global precipitation. *Int. J. Climatol.* **1990**, *10*, 111–127. [CrossRef]

9. Rubel, F.; Hantel, M. Correction of Daily Rain Gauge Measurements in the Baltic Sea Drainage Basin. *Nordic Hydrol.* **1999**, *30*, 191–208.

10. Becker, A.; Finger, P.; Meyer-Christoffer, A.; Rudolf, B.; Schamm, K.; Schneider, U.; Ziese, M. A description of the global land-surface precipitation data products of the Global Precipitation Climatology Centre with sample applications including centennial (trend) analysis from 1901–present. *Earth Syst. Sci. Data* **2013**, *5*, 921–998. [CrossRef]

11. Schneider, U.; Ziese, M.; Meyer-Christoffer, A.; Finger, P.; Rustemeier, E.; Becker, A. The new portfolio of global precipitation data products of the Global Precipitation Climatology Centre suitable to assess and quantify the global water cycle and resources. *Proc. IAHS Water Resour. Assess. Seas. Predict.* **2016**, *374*, 29–34. [CrossRef]

12. Trenberth, K.E.; Smith, L.; Qian, T.; Dai, A.; Fasullo, J. Estimates of the global water budget and its annual cycle using observational and model data. *J. Hydrometeorol.* **2007**, *8*, 758–769. [CrossRef]

13. Trenberth, K.E.; Fasullo, J.; Mackaro, J. Atmospheric moisture transports from ocean to land and global energy flows in Reanalyses. *J. Clim.* **2011**, *24*, 4907–4924. [CrossRef]

14. Rodell, M.; Beaudoing, H.K.; L'Ecuyer, T.S.; Olson, W.S.; Famiglietti, J.S.; Houser, P.R.; Adler, R.; Bosilovich, M.G.; Clayson, C.A.; Chambers, D.; et al. The observed state of the water cycle in the early twenty-first century. *J. Clim.* **2015**, *28*, 8289–8318. [CrossRef]

15. Hegerl, G.C.; Black, E.; Allan, R.P.; Ingram, W.J.; Polson, D.; Trenberth, K.E.; Chadwick, R.S.; Arkin, P.A.; Sarojini, B.B.; Becker, B.; et al. Challenges in quantifying changes in the global water cycle. *Bull. Am. Meteorol. Soc.* **2015**, *96*, 1097–1115. [CrossRef]

16. Carroll, M.L.; Townshend, J.R.; Di Miceli, C.M.; Noojipady, P.; Sohlberg, R.A. A new global raster water mask at 250 m resolution. *Int. J. Digit. Earth* **2009**, *2*, 291–308. [CrossRef]

17. ISLSCP II Land and Water Masks with Ancillary Data. Available online: http://dx.doi.org/10.3334/ORNLDAAC/1200 (accessed in January 2015).

18. World Meteorological Organization (WMO). *Climatological Normals (CLINO) for the Period 1961–1990*; WMO: Geneva, Switzerland, 1996.

19. Nicholson, S.E. An overview of African rainfall fluctuations of the last decade. *J. Clim.* **1993**, *6*, 1463–1466. [CrossRef]

20. Nicholson, S.E. The intensity, location and structure of the tropical rainfall belt over West Africa as a factor in interannual vaiability. *Int. J. Climatol.* **2008**, *28*, 1775–1785. [CrossRef]

21. Sanderson, M.G.; Hemming, D.L.; Betts, R.A. Regional temperature and precipitation changes under high-end (>= 4 °C) global warming. *Philos. Trans. R. Soc. A* **2010**, *369*, 85–98. [CrossRef] [PubMed]

22. Wang, B.; Wu, R.; Fu, X. Pacific-East Asian teleconnection: How does ENSO affect East Asian climate? *J. Clim.* **2000**, *13*, 1517–1536. [CrossRef]

23. Kumar, K.K.; Rajagopalan, B.; Hoerling, M.; Bates, G.; Cane, M. Unraveling the mystery of Indian Monsoon failure during El Nino. *Science* **2006**, *314*, 115–119. [CrossRef] [PubMed]

24. Adler, R.F.; Huffman, G.J.; Chang, A.; Ferraro, R.; Xie, P.; Janowiak, J.; Rudolf, B.; Schneider, U.; Curtis, S.; Bolvin, D.; et al. The Version-2 Global Precipitation Climatology Project (GPCP) monthly precipitation analysis (1979–present). *J. Hydrometeorol.* **2003**, *4*, 1147–1167. [CrossRef]

25. Adler, R.F.; Sapiano, M.; Huffman, G.J.; Bolvin, D.; Wang, J.J.; Gu, G.; Nelkin, E.; Xie, P.; Chiu, L.; Ferraro, R.; et al. New Global Precipitation Climatology Project monthly analysis product corrects satellite data shifts. *GEWEX News* **2016**, *26*, 7–9.

26. Vaughan, D.G.; Bamber, J.L.; Giovinetto, M.; Russell, J.; Cooper, A.P.R. Reassessment of net surface mass balance in Antarctica. *J. Clim.* **1999**, *12*, 933–946. [CrossRef]

27. De Couet, T.; Maurer, T. *Surface Freshwater Fluxes into the World Oceans*; Federal Institute of Hydrology (BFG): Koblenz, Germany, 2009.

28. Wilkinson, K.; von Zabern, M.; Scherzer, J. Global Freshwater Fluxes into the World Oceans. Available online: http://www.bafg.de/GRDC/EN/02_srvcs/24_rprtsrs/report_44.pdf?__blob=publicationFile (accessed on 10 January 2017).

29. Müller-Schmied, H.; Eisner, S.; Franz, D.; Wattenbach, M.; Portmann, F.T.; Flörke, M.; Döll, P. Sensitivity of simulated global-scale freshwater fluxes and storages to input data, hydrological model structure, human water use calibration. *Hydrol. Earth Syst. Sci.* **2014**, *18*, 3511–3538. [CrossRef]

30. Müller-Schmied, H.; Adam, L.; Eisner, S.; Fink, G.; Flörke, M.; Kim, H.; Oki, T.; Portmann, F.T.; Reinecke, R.; Riedel, C.; et al. Variations of global and continental water balance components as impacted climate forcing uncertainty and human water use. *Hydrol. Earth Syst. Sci.* **2016**, *20*, 2877–2898. [CrossRef]

31. Losev, K.S. Estimation of run-off from Antarctic and Greenland ice sheets. In Proceedings of the Symposium.on the Hydrology of Glaciers, Cambridge, UK, 7–13 September 1969; pp. 253–254.

32. Jacobs, S.S.; Helmer, H.H.; Doake, C.S.M.; Jenkins, A.; Frolich, R.M. Melting of ice shelves and the mass balance of Antarctica. *J. Glaciol.* **1992**, *38*, 375–387. [CrossRef]

33. Adam, J.C.; Lettenmaier, D. Adjustment of global gridded precipitation for systematic bias. *J. Geophys. Res.* **2003**, *108*, 4257. [CrossRef]

34. Osborne, J.M.; Lambert, F.H. The missing aerosol response in twentieth-century mid-latitude precipitation observations. *Nat. Clim. Chang.* **2014**, *4*, 374–378. [CrossRef]

35. Allen, M.R.; Ingram, W.J. Constraints on future changes in climate and the hydrologic cycle. *Nature* **2002**, *419*, 224–232. [CrossRef] [PubMed]

36. Kidd, C.; Becker, A.; Huffman, G.J.; Muller, C.L.; Joe, P.; Skofronick-Jackson, G.; Kirschbaum, D. So, How much of the earth's surface is covered by rain gauges? *Bull. Am. Meteorol. Soc.* **2017**, *98*, 69–78. [CrossRef]

37. Homepage of the Global Precipitation Climatology Centre (GPCC). Available online: http://gpcc.dwd.de (accessed on 10 January 2017).